Ground state of a dipolar fluid film

Mark Gross
Department of Physics and Astronomy, California State University, Long Beach, California 90840
(Received 8 June 1998)

The ground state of a simple dipolar fluid film is approximately determined as a function of the sample thickness and the volume fraction, for low volume fraction. A model involving analytic and numerical analysis is employed. The body-centered-tetragonal internal structure is found to be consistently lower in energy than face-centered-cubic. In the absence of polydispersity, the ground-state columns are approximately square in cross section. Interestingly, reflection symmetry breaking occurs due to the repulsion of the bound charges at the ends of the columns. A transition to a ''stripe'' phase is seen at higher volume fraction. The possibility is raised that the columnar structures seen in magnetorheological fluid experiments are far from equilibrium. [S1063-651X(98)01511-6]

PACS number(s): 68.15.+e, 61.20.Gy, 75.70.−i, 83.80.Gv

I. INTRODUCTION

One of the most interesting features of dipolar fluid systems is the richness of structures which can form, including chains, columns, and labyrinthine patterns. Columnar structures, in particular, are found at low volume fraction in electrorheological, magnetorheological (MR), and ferrofluid systems. The spacing and size of the columns can obey interesting scaling relations, although the scaling exponents appear to depend on certain details of the system [1–5]. The dynamics of column formation [6,7], particularly at very low volume fraction, are still not well understood. Even the interaction between two chains [8–11] turns out to be more complicated than was previously believed [12], at both zero and finite temperature.

Given the difficulty of carrying out a complete theoretical analysis of structure in dipolar fluids based on anything close to first principles, it is sensible to first address the most basic questions. Here we consider a model dipolar fluid without polydispersity and try to obtain information about the ground state. Rather crude approximations are made in order to simultaneously analyze the internal and external structure of the columns at low volume fraction. Accordingly, we consider this merely a first step toward more realistic calculations of structures at zero and finite temperature, in model and more realistic dipolar fluids, in equilibrium, and as a function of time.

Our study can be motivated from another point of view. Experiments on dipolar fluids are plagued by metastability and ''aging'' phenomena [13]. Thus there are questions which might be more easily attacked by a theoretical rather than an experimental approach. For example, the true ground state of a dipolar fluid is very difficult to determine experimentally. The system may get trapped in states which are not representative of the equilibrium phase. This is known to be the case at high volume fraction, and/or large sample thickness, and/or fast field ramping rates [14,15]. But it may also be the case at low volume fraction, modest sample thickness, and slow field ramping rates as well. Such would be the case, for example, if small columns were unable to coalesce into larger ones due to potential energy barriers. Determining the equilibrium state in such a case is not easy theoretically either, as one must cope with extremely rough potential energy landscapes. Still, in some cases the theoretical approach does seem somewhat more tractable. For example, one can analytically or numerically vary the column size and search for the one which minimizes the energy [4]. In such a way, one may hope to eventually determine which experimental results describe equilibrium phenomena and which are manifestations of metastability.

II. MODEL

A typical dipolar fluid column can easily consist of many thousands of dipolar particles. The columns, as well as the particles, exhibit long-range interactions, and so a serious numerical simulation designed to predict structure and its evolution from something close to first principles could easily require many millions of configuration updates, each of which requires computing billions of interactions between millions of particles. While impressive progress has been made along these lines [16], we are compelled by pragmatism and a desire to gain more physical insight, to consider models of structure in dipolar fluids. Many researchers have considered continuum models [1,4,17], and with significant success. But such models do not allow access of the internal structure. For example, whether columns are made up of particles in an approximately body-centered-tetragonal or face-centered-cubic structure is not a question which can be properly addressed in a continuum approach. Rather, in such models one is forced to treat quantities such as binding energy and surface tension in a phenomenological manner, fitting free parameters to experiment. While this is a useful and productive approach, here we consider an alternative line of attack in which the internal structure is accessible and there are no free parameters at all.

We now motivate and describe our model with which we try approximately to calculate the ground state of the simplest dipolar fluid film. By ''ground state'' we refer to the equilibrium state of the system at $\lambda \to \infty$. λ is the ratio of the maximum dipolar interaction energy of two particles to the thermal energy scale, $k_B T$. By ''the simplest dipolar fluid,'' we mean that all the particles will be taken to be spherical with the same radius and the same dipole moment (magni-

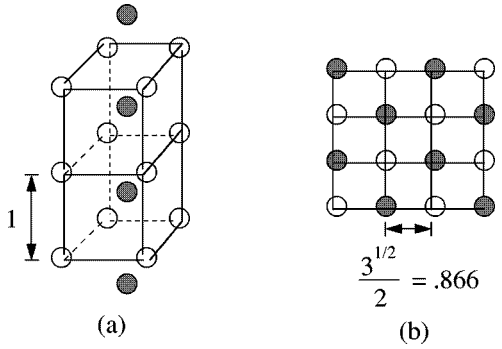

FIG. 1. (a) An ''exploded'' side view of the bct structure. Particles within a chain are actually in vertical contact. (b) The view from the top, after a rotation of 45°. In this paper, all distances are given in units of the particle diameter.

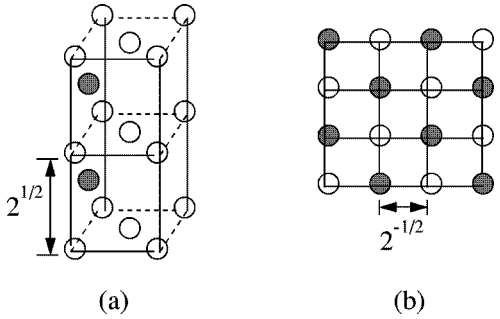

FIG. 2. (a) Exploded side view of the fcc structure with three shaded chains of particles left out for clarity of view. (b) The view from the top.

tude and direction). (Experimentally, this situation could be approximated using large superparamagnetic particles, if an external magnetic field is applied which is strong enough so that their induced magnetic moments reach saturation.) By ''film'' we mean that the sample thickness in the magnetic moment (vertical) direction is finite, typically on the order of hundreds of particle diameters, but the other dimensions are effectively infinite. We do not include mechanical forces associated with the interface between the sample and the boundary. Of course we admit that common laboratory fluids such as ferrofluids and MR fluids are more complicated than this. Yet we hope with this line of inquiry to eventually uncover some general truths of dipolar fluids which do not depend on their detailed and unique characteristics. At the least we hope to learn to ask the right questions. We also would like to build up our theoretical repertoire by starting with the most tractable situation.

To formulate the model, we are guided by results of experiments on somewhat similar systems, such as ferrofluids and ferrofluid emulsions [1–3]. In the ground state, at low volume fraction, we expect the columns to be identical and arranged in a perfectly hexagonal array. For the internal structure of the columns, we consider both body-centered-tetragonal (bct) [18–21] and a closed-packed, face-centered-cubic (fcc) structure [22]. Theoretical [18–20] and experimental [21] evidence has been given that bct is the approximate ground-state internal structure for ER fluids, in which the conductors at the boundary generate image dipoles out to infinity. Although we are more interested in the magnetic analog and therefore use no such boundary condition here, we should still expect that for a large enough sample thickness, bct will be the approximate ground-state internal column structure. We must point out that the exact ground-state internal structure of modest-sized columns cannot be expected to be exactly bct. An analog may be seen in the study of finite ionic clusters [23]. It is known that in the limit of an infinitely large ionic cluster, the bct structure has the lowest energy. However, it turns out that extremely large clusters are required before the structure becomes bct. Similarly, we must recognize the limitations of our considering only the bct and fcc internal structures for finite columns of dipolar particles. We hope to relax this limitation in a subsequent study.

Figure 1(a) shows an ''exploded'' side view of the bct structure, which can be formed from chains of spherical particles in *vertical contact*. The chains are then packed together laterally. Figure 1(b) shows the exploded view from the top, after a rotation of 45°. The shaded circles represent chains which are vertically shifted by a particle radius with respect to the chains represented by unshaded circles. The distance between nearest-neighbor chains is $\sqrt{3}/2$, in units of the particle diameter. *In this paper, all distances will be given in terms of the particle diameter.*

An exploded side view of a closed-packed fcc structure [22] is shown in Fig. 2(a), where three shaded chains consisting of face-centered particles have been left out for clarity of view. The dimensions of Fig. 2 are uniquely determined by requiring the particles to be in contact. Compared to the bct case, lateral packing has been increased at the expense of vertical packing: neighboring particles within a chain have a 41% gap in the vertical direction but chains are about 18% closer to their neighbors than in the bct structure of Fig. 1. In Fig. 2(b), as in Fig. 1(b), the shaded circles represent chains which are vertically shifted with respect to the chains represented by unshaded circles. In the fcc case the shift is $\sqrt{2}/2$. Note that the pattern of chains looks qualitatively the same in Figs. 1(b) and 2(b). This suggests that the only way to unambiguously distinguish these two structures by microscopic means (for example by freeze fracturing) would be to measure distances. The energy per particle for an infinite bct structure (Fig. 1) is smaller than the energy per particle for an infinite fcc structure (Fig. 2), but by less than 3%.

As we have discussed above, the individual particles present a formidable number of degrees of freedom to contend with, and so in our model we take the elementary degrees of freedom of our model to be uniform chains. These chains are assumed to be symmetric about the midplane of the sample. They are allowed to contain any number of particles up to the maximum number consistent with the boundary conditions and the lattice structure. For example, if the sample thickness is 64 (in units of the particle diameter), we allow the chains at ''even'' positions [represented, say, by the unshaded circles in Figs. 1(b) and 2(b)] to contain 0,2,4, . . . ,64 particles, whereas the ''odd'' chains can contain 0,1,3, . . . ,63 particles.

To find the ground state, we develop expressions for the approximate energy of any configuration. These are given in the next section. The approximation is quite accurate at low

volume fraction. We then use the method of simulated annealing to numerically minimize the energy and thereby determine the corresponding approximate ground-state configuration. A configuration is defined by where the chains are and the number of particles in each. Tapering of the columns occurs if the chains on the boundary have fewer particles than those near the center of a column. There is no need to put in a surface tension term by hand with a coefficient to be fitted as in continuum models. The different environment of the particles on the boundary of the columns effectively induces such a term in a natural way.

We found that there were many nearly degenerate low-energy states and it was therefore difficult to obtain the ''exact'' ground state (within the context of our model and our approximation of the energy of a configuration) for sample thicknesses larger than about 64. However, by performing runs with different maximum lateral sizes and shapes and comparing the lowest energy from different runs, we were able to determine a close approximation of the ground state, within the context of our model, even for much larger sample thicknesses.

III. ENERGY OF A CONFIGURATION

We now explain how we approximated the energy of each configuration. To keep things simple, we will derive expressions only for the bct internal structure. The energy expressions for a fcc configuration require minor rescalings of the formulas given below, associated with the different spacings in the vertical and lateral directions. (See above.) Expressions are simplified by using ''natural'' Gaussian units [10], which are just Gaussian units in which the dipole moment and the particle diameter are taken to be 1.

Let U be the energy per column. Recall that all columns are assumed to be identical in the ground state. U can be compartmentalized into three terms,

$$U = U_{\text{intra}} + U_{\text{inter}} + U_{\text{col}}. \tag{1}$$

U_{intra} is the intrachain energy associated with the particles within each chain of a column, U_{inter} is the interchain energy obtained by summing up contributions from each pair of chains within a column, and U_{col} is the interaction energy associated with one column and all other columns out to infinity.

Consider a uniform chain consisting of N particles in vertical contact. Call the internal energy of such a chain $u_{\text{intra}}(N)$. Summing over all chains which make up a column,

$$U_{\text{intra}} = \sum_{\text{chains}} u_{\text{intra}}(N),$$

where

$$u_{\text{intra}}(N) = \sum_{m>n} -\frac{2}{|m-n|^3} = -2\sum_{l=1}^{N-1} \frac{N-l}{l^3}.$$

$u_{\text{intra}} = 0$ for $N = 1$. For $N > 1$,

$$u_{\text{intra}} = -2.404\,113\,806\,319\,19N + \frac{\pi^2}{3} - \frac{1}{N} + \frac{1}{6N^3} - \frac{1}{10N^5} + \frac{5}{42N^7} - \frac{7}{30N^9},$$

to better than 0.01% accuracy. [The coefficient of N is $-2\zeta(3)$.] For a fixed volume fraction and sample geometry the ground state minimizes the total energy *per particle*. As u_{intra}/N is a monotonically decreasing function of N, the intrachain term attempts to make the chains (and therefore the columns) as long as possible, and so reduce tapering.

Now we turn to U_{inter}, the interaction energy associated with chains within a column. We may write this as a sum over pairs of chains within the column,

$$U_{\text{inter}} = \frac{1}{2}\sum_{i \neq j} u_{\text{inter}}(N_i, N_j),$$

where $u_{\text{inter}}(N_i, N_j)$ is the interaction energy associated with chains i and j which contain N_i and N_j particles, respectively. The energy associated with a pair of infinite, parallel, uniform dipolar chains has been known for a long time [18,12]. The corrections for the case of finite length chains of approximately the same length have also been calculated [10,11]. We now extend those calculations to chains of potentially quite different lengths, but with midpoints in the same lateral plane, the midplane of the sample. Such is the case for the model discussed above.

Let the two chains have N_i and N_j particles, respectively, and be a distance ρ apart in the lateral direction. Label the dipoles of chain 1 as $m = 1,2,\ldots,N_i$, and chain 2 as $n = 1,2,\ldots,N_j$. Let $\overline{N} \equiv (N_i + N_j)/2$, $\delta N \equiv (N_j - N_i)/2$, and $s = 0$ if $\overline{N}$ is an integer or $s = 1/2$ if $\overline{N}$ is half-integral. The interaction potential is

$$u_{\text{inter}} = \sum_{m=1}^{N_i}\sum_{n=1}^{N_j} \frac{\rho^2 - 2(n-m-\delta N)^2}{[\rho^2 + (n-m-\delta N)^2]^{5/2}}$$

$$= \sum_{l=-\infty}^{\infty} \frac{\rho^2 - 2(l-s)^2}{[\rho^2 + (l-s)^2]^{5/2}} (\overline{N} - \max(|\delta N|, |l-s|))$$

$$-2\sum_{l=\overline{N}}^{\infty} \frac{\rho^2 - 2l^2}{(\rho^2 + l^2)^{5/2}} (\overline{N} - \max(|\delta N|, l)).$$

Note that the last sum is over half-integers if $s = 1/2$. Using the Poisson summation identity on the first term and the Euler-MacLaurin formula on the second, we obtain an approximation which is quite accurate for $\overline{N} \gg 1$,

$$u_{\rm inter} \approx \sum_{m=-\infty}^{\infty} \int_{-\infty}^{\infty} dx\, \frac{\rho^2-2(x-s)^2}{[\rho^2+(x-s)^2]^{5/2}} (\bar{N}-\max(|\delta N|,|x-s|)) e^{2\pi i m x} - 2\int_{\bar{N}}^{\infty} dx\, \frac{\rho^2-2x^2}{(\rho^2+x^2)^{5/2}} (\bar{N}-x)$$

$$= 2\int_0^{\bar{N}} dx\, \frac{\rho^2-2x^2}{(\rho^2+x^2)^{5/2}} (\bar{N}-\max(|\delta N|,x)) + 2\sum_{m\neq 0} \cos(2\pi m s) \int_0^{\infty} dx\, \frac{\rho^2-2x^2}{(\rho^2+x^2)^{5/2}} (\bar{N}-\max(|\delta N|,x)) \cos 2\pi m x$$

$$= \frac{2}{\sqrt{(\delta N)^2+\rho^2}} - \frac{2}{\sqrt{\bar{N}^2+\rho^2}} + 4\sum_{m=1}^{\infty} \cos(2\pi m s) \int_0^{\infty} dx\, \frac{\rho^2-2x^2}{(\rho^2+x^2)^{5/2}} (\bar{N}-|\delta N|) \cos 2\pi m x$$

$$-4\sum_{m=1}^{\infty} \cos(2\pi m s) \int_{|\delta N|}^{\infty} dx\, \frac{\rho^2-2x^2}{(\rho^2+x^2)^{5/2}} (x-|\delta N|) \cos 2\pi m x$$

$$= \frac{2}{\sqrt{(\delta N)^2+\rho^2}} - \frac{2}{\sqrt{\bar{N}^2+\rho^2}} + 4(\bar{N}-|\delta N|) \sum_{m=1}^{\infty} \cos(2\pi m s)(2\pi m)^2 K_0(2\pi m \rho)$$

$$-4\sum_{m=1}^{\infty} \cos(2\pi m s) \int_{|\delta N|}^{\infty} dx\, \frac{\rho^2-2x^2}{(\rho^2+x^2)^{5/2}} (x-|\delta N|) \cos 2\pi m x.$$

The last term turns out to be numerically quite small for physical values of ρ (order 1 or bigger). Dropping it, and making a large $2\pi\rho$ expansion in the second-to-last term,

$$u_{\rm inter}(N_i,N_j) \approx \frac{2}{\sqrt{(\delta N)^2+\rho^2}} - \frac{2}{\sqrt{\bar{N}^2+\rho^2}} + \frac{8\pi^2}{\sqrt{\rho}} \min(N_i,N_j) e^{-2\pi\rho} \left[(\cos 2\pi s)\left(1-\frac{1}{16\pi\rho}\right) + (\cos 4\pi s) 2\sqrt{2} e^{-2\pi\rho} \right]. \quad (2)$$

This approximation to $u_{\rm inter}$ is typically accurate to within a few percent, even for chains which are in lateral contact.

There is a physical interpretation of the result. The first two terms represent the four monopole-monopole interactions associated with the bound charges at the ends of the chains. The denominators are the distances between the pairs of monopoles. The third term gives the approximate correction to the interaction energy associated with the discrete nature of the chains. We recognize this term as a minor generalization of the corresponding term for the case of two equal length chains [10,11]. The only substantive difference is that the common length of the two chains has been replaced by their overlap, $\min(N_i,N_j)$. Equation (2) also contains a better approximation to the sum over Bessel functions than given in Refs. [10,11], so as to provide a reasonably accurate approximation for chains which are in lateral contact.

What are the physical effects of the terms in Eq. (2), as regards the ground state of the system? The third term is responsible for the binding energy within columns. It attempts to increase the column thickness and reduce its tapering. (The column thickness should not be confused with the sample thickness. The former refers to the spatial extent of the column in the lateral direction, whereas the latter is the extent of the sample in the dipolar or z direction.) On the other hand, the first term, which dominates over the second term for nearby chains, tries to widely distribute the ends of the chains. We therefore expect it to attempt to reduce the thickness of the columns and to taper them, in order to spread out the bound surface charge as much as possible. The second term serves to limit the range of the first term by converting the interactions between chains from monopole-monopole to dipole-dipole at distances $\rho \sim \bar{N}$.

Finally we discuss the column-column interaction. We work in the low volume fraction regime in which the dominant interactions are between the bound monopole charges at the ends of the chains which make up the columns. We ignore the other terms, which fall off exponentially with the distance between the columns. Consider the pairs of monopole charges associated with two columns whose centers are a distance ρ apart. For some, the lateral separation is further apart than ρ, whereas for others it is closer. For low volume fraction we simply approximate all pairs to be ρ apart in the lateral direction. We also take the vertical (z) coordinate of the upper end of each chain equal to the average over the upper ends of all the chains which make up a column, and similarly for the lower ends. In this way, assuming a hexagonal pattern of columns as discussed above, we obtain the following crude approximation for the column-column interaction energy associated with any particular column:

$$U_{\mathrm{col}} \approx \frac{N_c^2}{2} \sum_{(m,n)\neq(0,0)} \left(\frac{2}{|m\vec{\rho}_1 + n\vec{\rho}_2|} - \frac{2}{\sqrt{|m\vec{\rho}_1 + n\vec{\rho}_2|^2 + (N_p/N_c)^2}} \right), \tag{3}$$

where N_p and N_c are the number of particles and the number of chains in a column, respectively, so that N_p/N_c is the average chain length of each column. Also

$$\vec{\rho}_1 \equiv d\left(\frac{\sqrt{3}}{2}, \frac{1}{2}\right) \quad \text{and} \quad \vec{\rho}_2 = d(0,1),$$

where d is the distance between nearest-neighbor columns. Note that we have summed over all pairs of columns out to infinity, to deal appropriately with the long-ranged column-column interaction.

Equation (3) can be rewritten as

$$U_{\mathrm{col}} \approx \frac{N_c^2}{d} S\left(\frac{N_p}{dN_c}\right), \tag{4}$$

where

$$S(r) \equiv 2 \sum_{m=0}^{\infty} \sum_{n=1}^{\infty} \left(\frac{1}{\sqrt{m^2+n^2+mn}} + \frac{1}{\sqrt{m^2+n^2-mn}} - \frac{1}{\sqrt{m^2+n^2+mn+r^2}} - \frac{1}{\sqrt{m^2+n^2-mn+r^2}} \right). \tag{5}$$

For $r \ll 1$ we can expand the summand in r to obtain

$$S(r) \approx \sum_{m=0}^{\infty} \sum_{n=1}^{\infty} \left\{ r^2 \left[\frac{1}{(m^2-mn+n^2)^{3/2}} + \frac{1}{(m^2+mn+n^2)^{3/2}} \right] - \frac{3r^4}{4} \left[\frac{1}{(m^2-mn+n^2)^{5/2}} + \frac{1}{(m^2+mn+n^2)^{5/2}} \right] + \frac{5r^6}{8} \left[\frac{1}{(m^2-mn+n^2)^{7/2}} + \frac{1}{(m^2+mn+n^2)^{7/2}} \right] \right\} \approx r^2(5.517\,088 - 2.535\,71r^2 + 1.936\,01r^4).$$

For $r \gg 1$, we use a variety of analytic and numerical methods to eventually obtain $S(r) \approx 4\pi r/\sqrt{3} - 4.213\,423 + 1/r$, where we have neglected terms which are exponentially small in r.

It is easy to check that the large and small r approximations overlap nicely in a region near $r = 0.67$, intersecting at $r \approx 0.669\,23$. Thus we can use the small r approximation for $r \leqslant 0.669\,23$ and the large r approximation for $r > 0.669\,23$:

$$S(r) \approx \begin{cases} r^2(5.517\,088 - 2.535\,71r^2 + 1.936\,01r^4), & r \leqslant 0.669\,23 \\ \dfrac{4\pi r}{\sqrt{3}} - 4.213\,423 + \dfrac{1}{r}, & r > 0.669\,23. \end{cases} \tag{6}$$

The crossover is quite smooth and the function is monotonically increasing for all r. The maximum disagreement with the exact sum (5) is at about the 2% level.

The volume fraction, ϕ, is of course related to the distance between nearest-neighbor columns, d. For a hexagonal array of columns,

$$\phi = \frac{\pi N_p}{d^2 t \sqrt{27}}, \tag{7}$$

where N_p is the number of particles in a column and t is the sample thickness. Inverting Eq. (7),

$$d = \sqrt{\frac{\pi N_p}{\phi t \sqrt{27}}} = 0.778 \sqrt{\frac{N_p}{\phi t}}. \tag{8}$$

Together, Eqs. (4), (6), and (8) provide an approximate expression for the column-column interaction energy associated with each column, for any configuration in our model.

As discussed above, the ground state minimizes the energy per particle for fixed volume fraction and sample geometry. An examination of the column-column interaction energy per particle using the expressions above shows that it is minimized by maximizing N_p/N_c and N_c. In order words, this interaction strives to increase the lengths of the chains and the number of chains in each column. It pushes the system in the direction of columns of maximal length, maximal thickness, and minimal tapering.

Taken together, we can see that the various terms which determine the energy of a configuration are in opposition and provide a rather complicated energy landscape as a function of column configuration. The repulsive monopole interaction within each column [first term of Eq. (2)] plays the role of spoiler, being the only term that tries to reduce the thickness of the columns and increase the tapering.

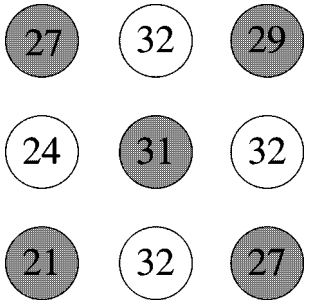

FIG. 3. Ground-state bct column structure for a volume fraction of 1% and a sample thickness of 32. Shown in a top-down exploded view are the numbers of particles in each chain which make up the column. Compare to Fig. 1(b).

We remind the reader that the expressions given in this section are for the bct internal column structure, and that minor rescalings are needed to adapt these formulas to the case of the fcc structure.

IV. RESULTS

Figure 3 shows the ground-state column configuration, assuming a bct internal structure, for a sample of thickness 32 (in units of the particle diameter), with a volume fraction of 1%. Each number shown is the number of particles in the chain at that location. Refer to Fig. 1(b) for this top-down view of the bct structure. The figure shows that the lowest energy bct configuration for a sample with 1% volume fraction and sample thickness 32 consists of precisely 9 chains, arranged in a square cross-sectional pattern, with each chain having the number of particles shown in the figure (27,32,29, . . .). In the bct structure the numbers must alternate between even and odd and they are bounded between 0 and the sample thickness. It should be emphasized that the number of chains, their locations, and their lengths were not put in by hand, but were found by minimizing the energy by the method of simulated annealing, within the context of our model, with the approximation as described in the preceding section.

Figure 4 is the bct ground state for a sample of thickness 64, with a volume fraction of 1%. In the cases of Figs. 3 and 4 we are confident that these are the exact ground states within the context of our model. We reached this conclusion by repeating our runs many times with many initial states.

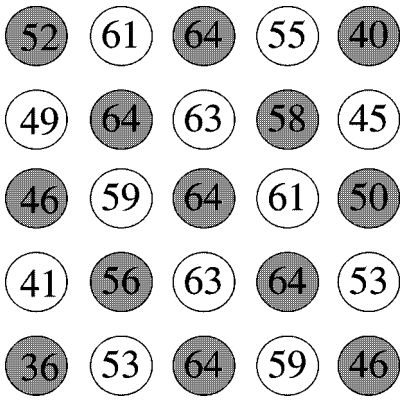

FIG. 4. Same as Fig. 3, but for a sample thickness of 64.

The states of Figs. 3 and 4 were reached several dozen times, but no lower energy configuration was ever encountered. For larger sample thicknesses (see below) the ground states appear to be close approximations to the true ground states, within the context of our model.

We first comment on some qualitative features of the configurations. Note the presence of facets as was suggested by Lobkovsky and Halsey [24]. The cross section of the column appears to exhibit the symmetry of the underlying bct structure, as would be expected. The reason column facets have not yet been seen experimentally may be an artifact of our model, or it may also be due to the effects of polydispersity, thermal effects, and metastability, all of which would tend to round out the cross sections of the experimental columns. Further work is needed to clarify this issue.

We also note the presence of tapering, a manifestation of the monopole-monopole interaction as discussed in the preceding section. For example, in Fig. 4 none of the 9 chains in the interior is composed of fewer than 56 particles, but 12 out of 16 of the chains on the boundary consist of fewer than 56 particles.

Despite the presence of facets, which appeared in our ground states for all values of volume fraction and sample thickness studied, note from Figs. 3 and 4 that the bct symmetry is broken, as the numbers shown are not invariant under reflection about a central horizontal axis or about either diagonal. Normally rotational invariance is broken down to a discrete subgroup through the formation of a perfect crystal. In this case, no remnant of rotational invariance remains, which is highly unusual for a ground-state crystalline structure. The origin of the symmetry breaking can be simply understood, however, as another manifestation of the monopole-monopole repulsion associated with the ends of the chains. As discussed in the preceding section, this energy term is reduced by staggering the positions of nearby ends as much as possible.

A final interesting feature, which we do not fully understand, is the presence of ''ridges,'' such as the central ridge in Fig. 4 in which all chains have the maximum number of particles allowed by the model. Similar ridges are seen in all our ground-state configurations at small volume fraction. They might be considered a precursor to the stripe or wall configurations seen at higher volume fraction. (See below.) Apparently the monopole-monopole interaction energy increase due to allowing the ends of the chains along *one plane* to be at approximately the same height is smaller than the decrease in the other energy terms which strive to maximize the chain lengths along that plane. Further investigation is needed to better understand this feature.

We now turn to a more systematic analysis of the data. Figure 5 shows the binding energy per particle as a function of sample thickness for a volume fraction of 1%. The binding energy is defined as the negative of the energy [Eq. (1)] in Gaussian units, where the particle diameter and the dipole moment of each particle are taken as 1. Equivalently, we may consider the binding energy to have been normalized by dividing by half of the potential energy of two particles in contact, with their dipole moments aligned along the axis of separation. Both axes of Fig. 5 (and all subsequent graphs) are therefore dimensionless; the abscissa is the sample thickness in units where the particle diameter is taken to be 1, or

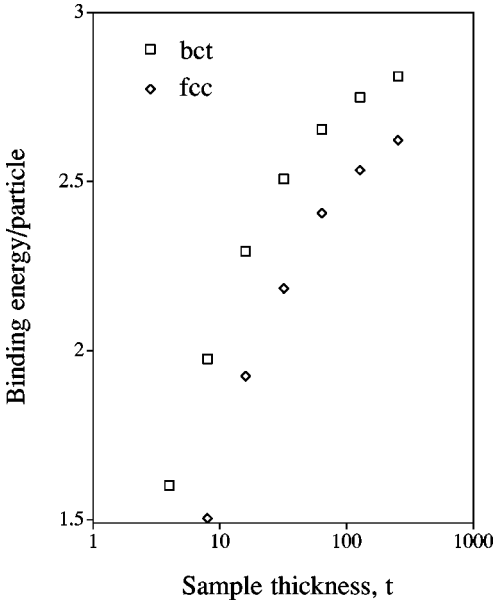

FIG. 5. Binding energy per particle versus sample thickness, for a volume fraction of $\phi = 0.01$. Results are for the bct and fcc structures, described in Sec. II.

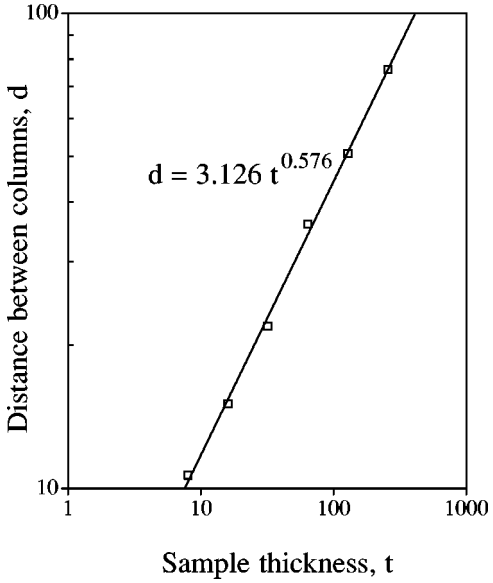

FIG. 7. Distance between nearest-neighbor columns versus sample thickness, for a volume fraction of $\phi = 0.01$.

equivalently, the sample thickness divided by the particle diameter. The main result of Fig. 5 is that the bct structure is consistently more stable than the fcc structure. The binding energy grows logarithmically with sample thickness for small thickness, and then begins to saturate at larger thickness. The difference in energy between an infinite bct structure and an infinite fcc structure is approximately 3% [18]. The values for $t = 256$ differ by about 6%.

Figure 6 shows the binding energy versus volume fraction with the sample thickness fixed to 64. Note that both the fcc and bct binding energies decrease linearly with volume fraction. The decrease is associated with the monopole-monopole interaction which, because it falls off only inversely with distance (for distances much less than the chain length), plays a successively larger role the more tightly the chains are packed. In Fig. 6 we see again that the bct structure is consistently more stable. Accordingly, as we are concerned with the approximate ground state of the dipolar fluid, the rest of our results will focus solely on the bct structure.

In Fig. 7, we plot the distance between nearest-neighbor columns versus sample thickness for volume fraction 1%. The dependence is a power law, as has been found many times experimentally and theoretically [1–4,12,5]. Unfortunately the power does not appear to be universal but depends on the dipolar system being considered. For our model the exponent is approximately 0.576 in the range of sample thicknesses considered.

Figure 8 shows the thickness of the columns, defined as the square root of the number of chains, versus sample thick

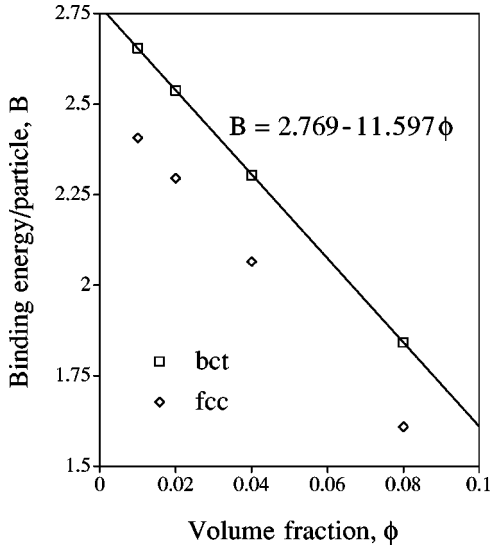

FIG. 6. Binding energy per particle versus volume fraction, for a sample thickness of 64. Results are for the bct and fcc structures described in Sec. II.

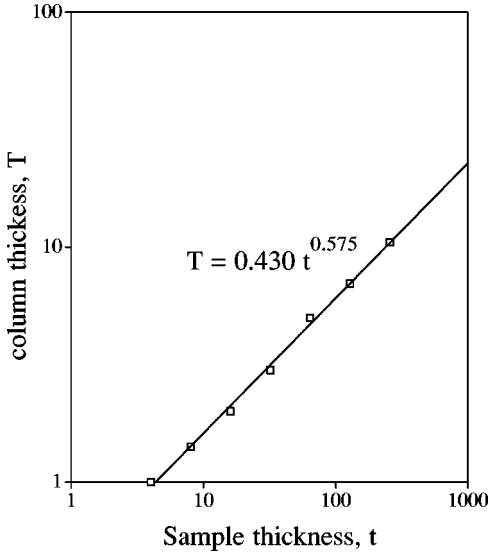

FIG. 8. Column thickness versus sample thickness for a volume fraction of $\phi = 0.01$.

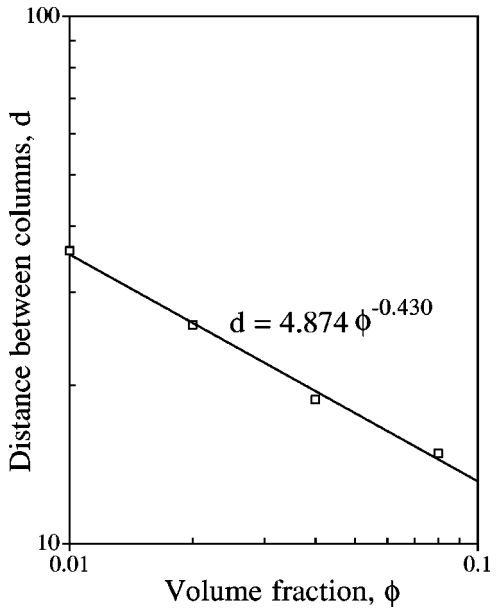

FIG. 9. Distance between nearest-neighbor columns versus volume fraction for a sample thickness of 64.

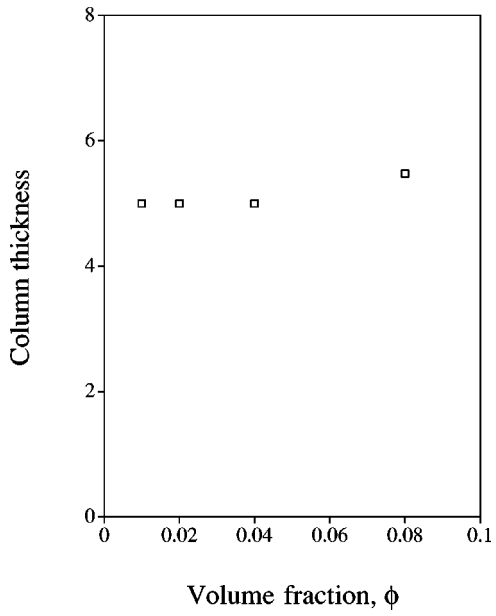

FIG. 10. Column thickness versus volume fraction for a sample thickness of 64.

ness for volume fraction 1%. Again the dependence is a power law, and the power is essentially the same as in Fig. 7. By Eq. (8), this implies that for fixed volume fraction, the average chain length increases in proportion to the sample thickness. The fact that the columns get thicker as the sample thickness increases is easily understood in terms of the decreasing significance of the monopole-monopole interaction energy, which does not grow with the chain length. This is the only energy term which tends to decrease the column thickness. Thus as the sample thickness increases, the monopole-monopole interaction becomes relatively less important, and so the column thickness increases. The power-law dependence of column thickness on sample thickness is similar to that obtained by Halsey and Toor in a continuum model of ER fluid [12]. They obtained an exponent of 2/3.

Figure 9 is a plot of the distance between nearest-neighbor columns versus volume fraction for a sample thickness of 64. We see that the distance decreases with volume fraction in an approximate power-law fashion.

Figure 10 shows the column thickness versus volume fraction for a sample thickness of 64. We see little dependence for a small volume fraction. Together, Figs. 9 and 10 indicate that as more particles are added to the sample, the lateral thickness of the columns stays relatively constant, while the distance between them decreases roughly as $\phi^{-1/2}$, consistent with Eq. (8). Significant deviations from this situation appear as the volume fraction increases. As the volume fraction exceeds 0.08, a phase transition to a stripe phase occurs, as discussed below.

In Fig. 11, a semilogarithmic plot of the tapering fraction versus sample thickness for volume fraction $\phi=0.01$ is displayed. Tapering fraction f is defined as

$$f=1-\frac{N_p}{tN_c}, \tag{9}$$

where N_p and N_c are the number of particles and chains, respectively, which make up a column, and t is the sample thickness. We see that the tapering fraction increases roughly logarithmically with sample thickness, starting out near zero for the smallest columns associated with the smallest sample thicknesses.

Figure 12 shows the tapering fraction versus volume fraction for a sample thickness of 64. The tapering fraction decreases linearly as the volume fraction increases until, at a volume fraction between 0.08 and 0.09, the tapering fraction appears to go abruptly to zero (or nearly so), and we find an apparent *phase transition to a stripe state*, as was predicted earlier [4,17]. In this phase, ''walls'' rather than columns appears to be the ground-state structure. We inferred this

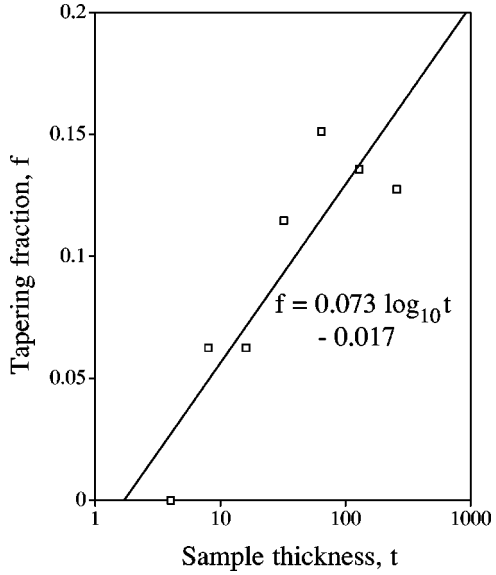

FIG. 11. Tapering fraction versus sample thickness, for a volume fraction of $\phi=0.01$.

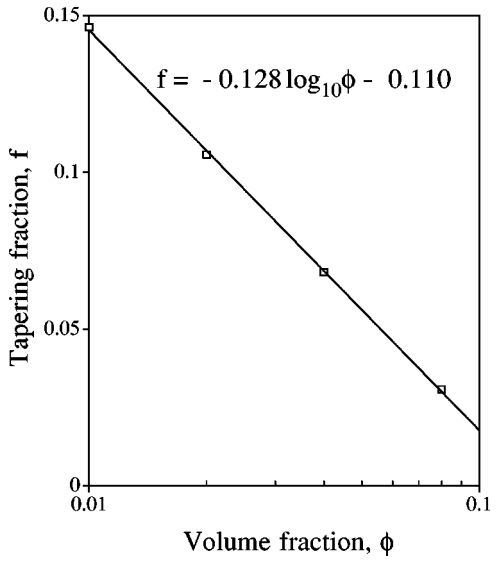

FIG. 12. Tapering fraction versus volume fraction, for a sample thickness of 64.

transition from the fact that, for $\phi \geq 0.09$, if one transverse dimension of the ''column'' was held fixed, the energy of the structure continually decreased as the other transverse dimension was allowed to increase. No such behavior occurs for $\phi \leq 0.08$. It should be kept in mind that in our model, low volume fraction and a periodic hexagonal structural pattern are assumed, and only the structure within each hexagonal cell is determined by minimizing the energy. Therefore we can only estimate the location of the column to stripe phase transition from the low volume-fraction side. A more accurate analysis of the transition to the stripe phase could be obtained by comparing energies obtained in our model to energies obtained in a separate model which *a priori* constructs a striped state.

Apparently there has been no conclusive experiment demonstrating that the stripe phase of MR fluids is the ground state at sufficiently high volume fraction. So-called ''bent wall'' or ''labyrinthine'' metastable structures are obtained without shear [14], but these are believed to be metastable states. With shearing, the stripe phase can be induced [25], and it does not dissipate when the shearing stops. The work presented here provides some additional evidence that it may be the true ground state for a high volume fraction.

V. SUMMARY AND DISCUSSION

We examined the ground-state structure of a dipolar fluid film via a model which made the internal structure of the columns accessible and involved no free parameters. While the model involved several simplifications, making precise comparison to present experiments difficult, columns involving up to tens of thousands of particles were able to be considered and several interesting phenomena were observed. It was found that the bct structure was lower in energy than a comparison fcc structure. With no polydispersity or thermal effects, columns were found to have an approximately square cross section and exhibit tapering. Yet reflection symmetries were found to be broken due to the monopole-monopole interaction. Each ground-state column exhibited a central ''ridge,'' which has not been satisfactorily understood.

Plots of energy, intercolumn distance, column thickness, and column tapering versus sample thickness and volume fraction have been displayed and discussed. An abrupt phase transition from a columnar to a stripe phase was observed at a volume fraction between 8% and 9%.

It is a fact that the ground-state columns of this theoretical investigation were found to be significantly thicker than experimental columns of MR fluids (for corresponding sample thicknesses) obtained by raising the external magnetic field very slowly to a high value, in order to approach an equilibrium state [2,3]. Although the reason may well have to do with differences between our model and the experimental system, we put forth another speculative suggestion here, first alluded to in the introductory section. Columns repel each other at large distances and are able to coalesce only at short distances, even when coalescence is energetically favorable. For low volume fraction and large field, the potential energy barrier for column aggregation may not be able to be overcome over laboratory time scales. In other words, we speculate that the column sizes seen in Refs. [2,3] *may*, unavoidably, not be representative of the equilibrium structure.

We hope to reexamine many of the features of this preliminary work in a more fundamental treatment of dipolar fluids to follow. At this point our most firmly established result may be that despite numerous careful experiments and detailed calculations and simulations, our understanding of the structure of dipolar fluids is still in its infancy.

Note added. A preliminary version of this work was presented at a meeting of the American Physical Society [Bull. Am. Phys. Soc. **43**, 652 (1998)]. Some overlapping results were presented at the same session by P. Sheng [Bull. Am. Phys. Soc. **43**, 652 (1998)] and the latter were published in Physical Review Letters [L. Zhou, W. Wen, and P. Sheng, Phys. Rev. Lett. **81**, 1509 (1998)].

ACKNOWLEDGMENTS

The author would like to thank Jing Liu and Robijn Bruinsma for useful early discussions. This work was supported by Grant No. CC4327 from the Research Corporation, Grant No. DMR-9803618 from the National Science Foundation, and by California State University.

[1] H. Wang, Y. Zhu, C. Boyd, W. Luo, A. Cebers, and R. E. Rosensweig, Phys. Rev. Lett. **72**, 1929 (1994).

[2] J. Liu, E. M. Lawrence, A. Wu, M. L. Ivey, G. A. Flores, K. Javier, J. Bibette, and J. Richard, Phys. Rev. Lett. **74**, 2828 (1995).

[3] E. Lawrence, M. Ivey, G. A. Flores, J. Liu, J. Bibette, and J. Richard, Int. J. Mod. Phys. B **8**, 2765 (1994).

[4] A. Cebers, in *Magnetic Fluids and Applications Handbook and Database*, edited by B. Berkovsky (Begell House, New York, 1996), and references therein.

[5] E. Lemaire, Y. Grasselli, and G. Bossis, J. Phys. II **2**, 359 (1992); E. Lemaire, G. Bossis and Y. Grasselli, *ibid.* **4**, 253 (1994).
[6] J. E. Martin, J. Odinek, and T. C. Halsey, Phys. Rev. Lett. **69**, 1524 (1992).
[7] Y. Zhu, E. Haddadian, T. Mou, M. Gross, and J. Liu, Phys. Rev. E **53**, 1753 (1996).
[8] A. S. Silva, R. Bond, F. Plouraboué, and D. Wirtz, Phys. Rev. E **54**, 5502 (1996).
[9] M. Mehrdad, N. Jamasbi, G. A. Flores, and J. Liu, in *Proceedings of the 6th International Conference on Electrorheological Fluids, Magnetorheological Suspensions and Their Applications*, edited by M. Nakano (World Scientific, Singapore, in press).
[10] M. Gross and S. Kiskamp, Phys. Rev. Lett. **79**, 2566 (1997).
[11] M. Gross, S. Kiskamp, H. Eisele, Y. Zhu and J. Liu, in *Proceedings of the 6th International Conference on Electrorheological Fluids, Magnetorheological Suspensions and Their Applications* (Ref. [9]).
[12] T. C. Halsey and W. Toor, Phys. Rev. Lett. **65**, 2820 (1990); J. Stat. Phys. **61**, 1257 (1990).
[13] T. Jonsson, J. Mattsson, C. Djurberg, F. A. Khan, P. Nordblad, and P. Svedlindh, Phys. Rev. Lett. **75**, 4138 (1995).
[14] G. Flores and J. Liu, in *Proceedings of the 6th International Conference on Electrorheological Fluids, Magnetorheological Suspensions and Their Applications* (Ref. [9]).
[15] G. A. Flores, J. Liu, M. Mohebi, and N. Jamasbi (unpublished).
[16] J. E. Martin, R. A. Anderson, and C. P. Tigges, J. Chem. Phys. **108**, 3765 (1998); **108**, 7887 (1998).
[17] T. C. Halsey, Phys. Rev. E **48**, R673 (1993).
[18] R. Tao and J. M. Sun, Phys. Rev. Lett. **67**, 398 (1991).
[19] R. Tao and J. M. Sun, Phys. Rev. A **44**, R6181 (1991).
[20] R. Tao and Q. Jiang, Phys. Rev. Lett. **73**, 205 (1994).
[21] T. Chen, R. N. Zitter, and R. Tao, Phys. Rev. Lett. **68**, 2555 (1992).
[22] T. C. Halsey and W. Toor, Phys. Rev. Lett. **65**, 2820 (1990).
[23] J. Schiffer, Science **279**, 675 (1998), and references therein.
[24] A. E. Lobkovsky and T. C. Halsey, J. Chem. Phys. **103**, 3737 (1995).
[25] S. Cutillas, G. Bossis, and A. Cebers, Phys. Rev. E **57**, 804 (1998).